Materials Letters 170 (2016) 122–125

Contents lists available at ScienceDirect

Materials Letters

journal homepage: www.elsevier.com/locate/matlet

Fabrication and characterization unique ribbon-like porous Ag/$LaFeO_3$ nanobelts photocatalyst via electrospinning

Shudan Li*, Yun Zhao, Chenyi Wang, Doudou Li, Kun Gao

School of Chemistry and Materials Science, Shanxi Normal University, Linfen 041004, China

ARTICLE INFO

Article history:
Received 23 November 2015
Received in revised form
17 January 2016
Accepted 4 February 2016
Available online 11 February 2016

Keywords:
Ag/$LaFeO_3$
Nanobelts
Ribbon-like porous
Photocatalyst
Microstructure

ABSTRACT

Ag/$LaFeO_3$ nanobelts were synthesized by a sol-gel assisted electrospinning method. The surface morphology, microstructure and crystal structure were investigated by scanning electron microscopy and X-ray diffraction respectively. The SEM results reveal that the obtained Ag/$LaFeO_3$ nanobelts contain a large number of pores. The XRD analysis shows that when Ag content reaches 15 wt%, there are obvious Ag° characteristic peaks. With the increase of Ag content, Ag° and $LaFeO_3$ characteristic peaks in the samples are enhanced as well. The photocatalytic activity of Ag/$LaFeO_3$ nanobelts is investigated for the photo-degradation of Rhodamine B aqueous solution under visible light. The result demonstrates that 15 wt% Ag/$LaFeO_3$ nanobelts exhibit excellent photocatalytic activity compared with others.

1. Introduction

Due to the rapid development of modern society, a large amount of organic or inorganic pollutants engender along with the ever worsening environmental issues [1,2]. Compared with traditional catalysts, the perovskite materials have attracted extensive attention because of its nontoxic, high-efficiency, high thermal stability and unique physicochemical property [3–5]. $LaFeO_3$, as the most typical perovskite-type oxide, has gained people's approval and is considered to be one of the greatest developmental potential photocatalyst materials [6,7]. However, the conditions which need to utilize these semiconductor photocatalysts, such as UV irradiation, restrict their applications in reality [8]. Introducing a small fraction of noble metal nanoparticles (NPs), such as silver, as a conductive additive is a fascinating concept to address this inadequacy and improve properties [9,10]. In order to improve the practical applicability of the photocatalyst, Ag/$LaFeO_3$ nanocomposites are synthesized by chemical or physical processes for two purposes. The first is to extend the light adsorption spectrum and improve the efficiency of light utilization. Second, suppress the recombination of photogenerated electron/hole pairs which weaken the function of the photocatalyst [11–13]. Nanocomposites $LaFeO_3$ coupled with Ag can enhance their photocatalytic efficiency as a result of the synergistic effect on photocatalytic properties. The Ag/$LaFeO_3$ nanocomposites not only improve the separation efficiency between the photogenerated electrons and electron holes, but also introduce both impurity and defect levels to the forbidden band of $LaFeO_3$ [14].

To the best of our knowledge, reports on the preparation of Ag/$LaFeO_3$ nanobelts via a sol-gel assisted electrospinning method are still limited. In this work, we developed a simple and scalable process for obtaining continuous porous Ag/$LaFeO_3$ nanofibers by sol-gel assisted electrospinning method of $La(NO_3)_3$/$Fe(NO_3)_3$/$AgNO_3$/PVP precursor solution with ethanol and acetic acid as the only one solvent.

2. Experimental

2.1. Fabrication of Ag/$LaFeO_3$ nanobelts

The nanobelts perovskite oxides of Ag/$LaFeO_3$ were synthesized by a sol-gel assisted electrospinning method. The reagents used were analytic grade of $La(NO_3)_3$, $Fe(NO_3)_3$, $AgNO_3$, PVP powder, ethanol and acetic acid. Firstly, the required metal salts were added to a mixture of 11 mL ethanol and 1 mL acetic acid, followed by vigorous stirring for 30 min. Then 3.8 g PVP powder was added to the above solution, and the mixture was continuously stirred for another 10 h to obtain a sol-precursor solution. The molar ratio of $La(NO_3)_3$ to $Fe(NO_3)_3$ was 1:1. Ag content is 5 wt%, 10 wt%, 15 wt% and 20 wt%, which were designated as sample a, b, c and d, respectively. 10 mL of the precursor solution was loaded into a 20 mL

* Corresponding author.
E-mail addresses: lishudan0451@163.com (S. Li), gaokun0451@163.com (K. Gao).

http://dx.doi.org/10.1016/j.matlet.2016.02.014
0167-577X/

syringe with the outer one of the coaxial needle. A high-voltage supply was connected to the inner needle to obtain electrostatic spinning fibers. The solution was pumped continuously using a syringe pump at a rate of 0.4 mL h^{-1} at an applied voltage of 16 kV. A sheet of aluminum foil, which was 15 cm away from the needle point, was used as the collector. Finally, the obtained composite nanofibers were calcined at 500 °C for 2 h in air to obtain the $Ag/LaFeO_3$ nanobelts with a heating rate of 2 °C min^{-1}.

2.2. Characterization

XRD patterns were collected on Ultima IV (Rigaku) diffractometer using Cu Kα radiation (40 kV, 40 mA). The SEM images were taken by a JEOL JSM-6700F field emission SEM instrument.

2.3. Photocatalytic activity

The photocatalytic activity evaluation of $Ag/LaFeO_3$ nanobelts for the photo-degradation of Rhodamine B (Rh B) aqueous solution was carried out in a home-built reactor at ambient temperature. A 125 W high-pressure fluorescent Hg lamp was used as the light source. For each run, 0.1 g $Ag/LaFeO_3$ nanobelts were dispersed in 50 mL Rh B solution with a concentration of 10 mg L^{-1}. Prior to the beginning of illumination, the reactor contents were allowed to equilibrate in the dark with stirring for 20 min. Absorbance of irradiated samples was determined with a Perkin Elmer fLambda 900 UV/vis/NIR spectrometer immediately after irradiation and removal of the $Ag/LaFeO_3$ nanobelts. The photocatalytic performance of the obtained $Ag/LaFeO_3$ nanobelts was contrasted with $LaFeO_3$ nanobelts.

3. Results and discussion

Fig. 1 shows the SEM images of the as-electrospun composite fibers. The diameter of sample a is not uniform and it appears wrinkling and collapse on the surfaces of the fibers. This is attributed to the interference of the inner needle and the uneven distribution of the metal ions in the fibers [15]. Interestingly, in terms of fibers morphology, the results reveal that composite fibers transform systematically from cylindrical fibers to belt shape with the increasing amount of Ag content. Samples a and b exhibit wrinkled composite fibers, while samples c and d display belt composite fibers. When Ag content is 20 wt%, the thickness of the ribbon fiber is minimal. That may be because when the solution after the salt content increases, the viscosity of the precursor solution is also increased, the electric field strength cannot overcome the viscous force of the solution, so the fibers cannot easily be stretched into a linear shape but produce belt. Meanwhile, the concentration of the charged ions in the solution increases, the role of mutual exclusion would increase and the jet becomes unstable, affecting the distribution of ions in the fibers and forming belt fiber ultimately.

Fig. 2 displays the SEM images of $Ag/LaFeO_3$ nanobelts after calcination. From Fig. 2, it can be observed that four different nanofibers after calcination exhibit good nanobelts with highly porous structure. When the high-voltage connect to the inner needle, the electropositive nature drives the metal ions in the solution are diffuse from the core to the surface. During the formation of $LaFeO_3$ crystallites, bidirectional concentration gradients for Fe^{3+} and La^{3+} and $LaFeO_3$ crystallites exist in the cross section of nanofibers, which would drive the metal ion to diffuse from the core to the surface, and $LaFeO_3$ particles from the surface to the core to the nanofiber. When the temperature reaches the decomposition temperature of PVP, the PVP components are decomposed completely to product a lot of gas. The gas escape from the nanofiber wall destroying the structure of the nanofiber to fabricate nanobelts. Eventually it remains the belt structure and the surface of the nanobelts is fill of small holes. When Ag content is 5 wt% and 10 wt%, the width of the nanobelts is not uniform. However, when Ag content is 15 wt% and 20 wt%, the nanofibers exhibit good morphology and the width of the nanobelts is uniform.

Fig. 3 shows XRD patterns of the $Ag/LaFeO_3$ nanobelts. As it can be seen from Fig. 3, when the Ag content is less than 10 wt%, only

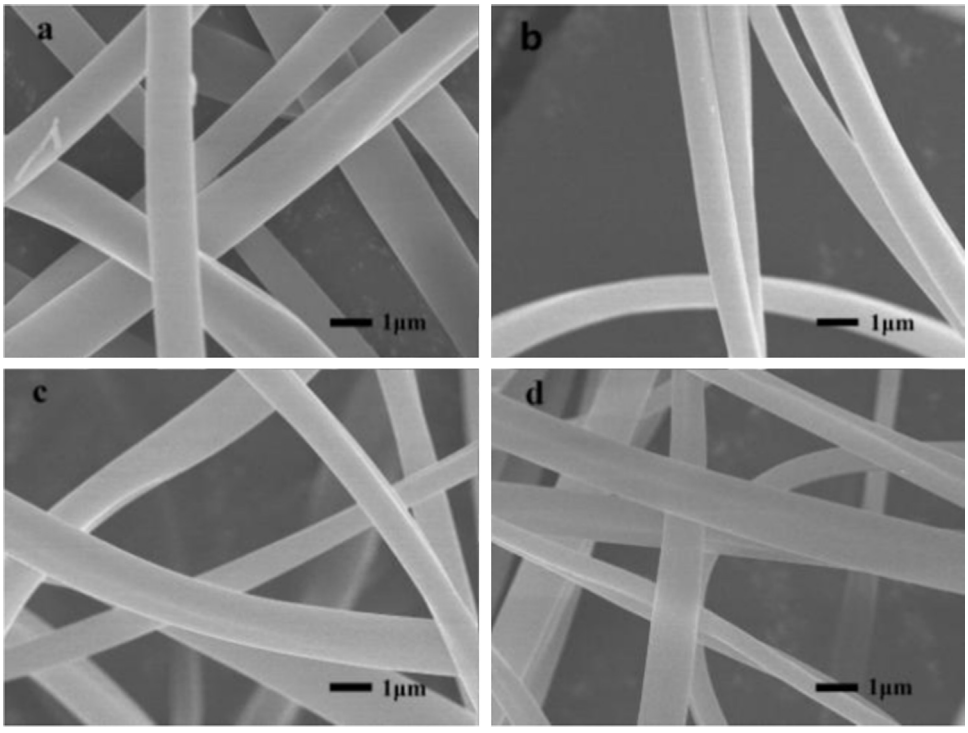

Fig. 1. SEM images of composite fibers with different Ag contents.